archives
of thermodynamics
Vol. **39**(2018), No. 1, 129–145
DOI: 10.1515/aoter-2018-0007

Experimental observations of flow structures during DEP controlled boiling in a microchannel

MARCIN LACKOWSKI*
ROMAN KWIDZIŃSKI
JAROSŁAW KARWACKI
TOMASZ PRZYBYLIŃSKI

Institute of Fluid Flow Machinery Polish Academy of Sciences, Fiszera 14, 80-231 Gdańsk, Poland

Abstract The paper presents results of experimental investigation of microchannel boiling flow which was controlled by dielectrophoretic (DEP) restrictor. The DEP restrictor was connected to the microchannel liquid supply tube. Operation of DEP restrictor influenced the flow rate at the microchannel inlet. Resulting changes in flow structures and vapour content along the microchannel were observed and analysed with a high-speed video camera. Video recordings were synchronised with measurements of differential pressure between the channel inlet and outlet. It was found that it is possible to change average void fraction in the microchannel by switching on and off the voltage applied to the restrictor electrodes. However, to achieve significant variation of the void fraction, applied voltage should be of the order of 2000 Vpp. The voltage switching also generates oscillations of the differential pressure. The amplitude of these oscillations is proportional to the voltage magnitude, reaching 35 Pa for 2400 Vpp.

Keywords: Visualisation; Liquid dielectrophoresis; Flow control; Flow structures

1 Introduction

Low-boiling temperature fluids are more and more commonly used not only in refrigeration technology and heat pump applications, but also in a widely

*Corresponding Author. Email: mala@imp.gda.pl

understood distributed power engineering (including electricity generation systems based on Rankine cycles). Most of the low-boiling fluids are dielectrics.

On the other hand, microchannel heat exchangers are increasingly being used in many fields of industry and science. Controlling the flow and the boiling process in individual microchannels is one of the most important issues. Among the techniques that can be used to control the flow rate in microchannels, there are methods based on the effect of the electric field on a flowing liquid. This effect is of particular importance in the case of dielectric liquids.

Devices, which operating principles are based on such phenomena as electrocapillarity, electrowetting or dielectrophoresis [1–5], provide the ability to control the movement of particles, droplets or liquids in the electric field. One of the first and most significant experiments in this area of research is Pelat's experiment described in [6], which became the basis for the analysis conducted by Jones [7–8] – who named the phenomenon he had observed as 'liquid dielectrophoresis' (LDEP). Pellat's experiment showed that the electric field generated between two parallel flat electrodes causes an increase in the liquid level as the voltage applied to the electrodes increases.

The LDEP, the above-mentioned phenomenon discovered by Pellat, was used in an original device designed to control the flow rate in microchannels [9–10]. According to the authors' knowledge, this is the first and so far the only use of the dielectrophoresis phenomenon to control the flow rate at such a magnitude that it could possibly be applied to systems equipped with microchannel heat exchangers. Below is a brief description of the flow controller (restrictor) operation.

The test controller consists of a microchannel with walls made of copper and spacing of 0.2 mm. The length of the microchannel is 10 mm which is equal to the electrodes' width. The microchannel walls are formed by electrodes to which the voltage is applied. Furthermore, there is a flow limiter at the microchannel inlet in the form of an opening at the bottom edge of the microchannel. Through this opening, having a height of 200 μm, the liquid flows into the flow controller and into the area between the electrodes to which the voltage is applied. The voltage causes an increase in the level of liquid in the space between the walls of the controller. Changes in the liquid level between the electrodes affect the flow rate of the liquid flowing through an opening forming the controller outlet. The effect of the voltage

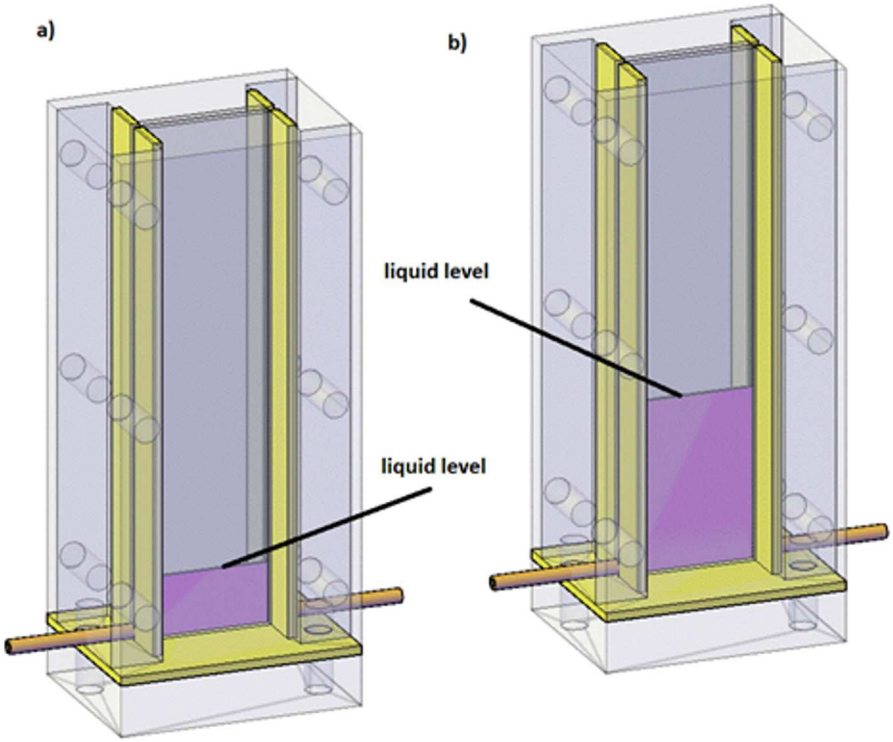

Figure 1: Comparison of the liquid level in the controller both in the presence and absence of the applied voltage: a) without electric field, b) with electric field.

applied to the microchannel walls (electrodes) is illustrated in Fig. 1. For the width of the control channel used in these tests the applied voltages ranged from several hundreds to about 1200 V. The liquid level between the walls of the controller microchannel changes proportionally to the voltage applied to these walls: the higher the voltage, the higher the liquid level.

The phenomenon of the liquid level rise within the inter-electrode area – caused by the electric field acting on the molecules of this liquid – is the basic operating principle of the flow controller which is connected upstream of the inlet to the heated microchannel in which boiling is to be observed.

The subject of the research, the results of which are reported hereafter, is the use of the described device to control the flow in the heated microchannel. In the experimental studies, the main focus was at the influence of the voltage applied to the walls (electrodes) of the controller on the boiling process in the heated microchannel and the optical observation

and analysis of structures evolving during this process. Detailed analysis of transient boiling mechanisms is omitted here but can be found in the papers of other researchers, e.g., in [11–13].

2 Experimental methods

The impact of a dielectrophoretic flow controller (restrictor) on the boiling process in a microchannel was investigated on the test rig shown in Fig. 2.

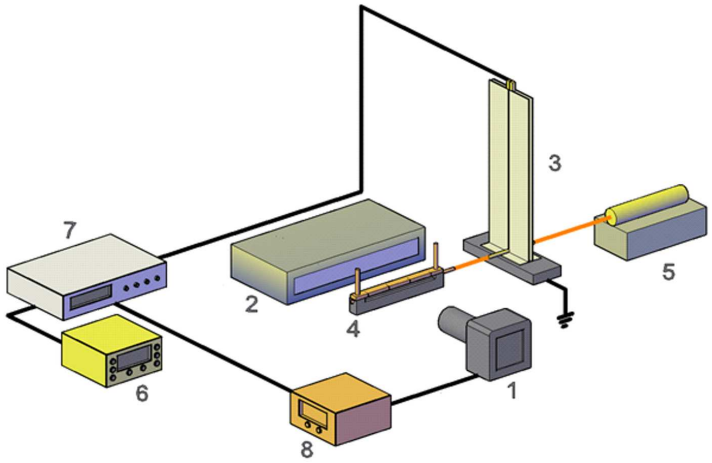

Figure 2: Schematic view of the experimental test rig: 1 – high-speed camera (Microtron MC1310), 2 – linear type light-emmitig diode lighting devices (CCS LNSP-200 SW), 3 – flow controller (restrictor), 4 – heated microchannel, 5 – precise programmable pump, 6 – arbitrary generator, 7 – high voltage amplifier, 8 – monitoring and control system.

It comprises an arbitrary waveform generator (Rigol DG1032Z) and a high-voltage power amplifier (Trek 10/10B-HS). The generated voltage is then applied to the electrodes of the dielectrophoretic flow rate control system. The flow in the boiling microchannel is generated by a modular syringe pump (Chemyx Fusion 200). This microchannel has a length of 130 mm and a square cross-section of 400×400 μm^2. It was machined in a transparent polycarbonate plate with one wall made of Inconnel foil. A thermal flux is supplied to the microchannel in a controlled manner by electrical heating of the foil, using a direct current adjustable power supply (Powerlab 3030D).

A high-speed camera (Microtron MC1310) equipped with a Schneider Xenoplan 2.0/28-0901 lens and an image acquisition board (NI NI PCIe-1429) in Full Camera Link configuration were used for observing and recording of the flow structures. A set of linear type light-emmitting diode (LED) lighting devices (CCS LNSP-200 SW) provided illumination of the flow structures in the channel. Six thermocouples (model TP-221K-B-200, manufactured by Czaki Thermo-Product) were used for temperature measuring, while the Endress+Hauser Deltabar S PMD75 differential pressure transmitter measured the pressure difference between the microchannel inlet and outlet. At the start of each measurement session, the pressure transmitter readings were adjusted to indicate zero during a stationary liquid-only flow in the microchannel at slightly undersaturated temperature. The data acquisition system is based on NI SCXI-1000 signal conditioning modules fitted with measuring and control cards. It provides a continuous collection of data, which is particularly important given the dynamic character of the processes under investigation.

The measurement accuracies were $\pm 0.35\%$ for the flowrate and ± 0.2 K for temperature. For the pressure measurement, the transmitter span was set to ± 200 Pa and the accuracy was $\pm 0.035\%$ of the span. Working fluid was isopropyl alcohol (2-propanol). Its boiling took place under near-atmospheric pressure as the microchannel outlet and the restrictor electrodes were open to the ambient (normal boiling point is 355.4 K). The pump flowrate and heating power were kept constant during a measurement acquisition.

3 Experimental results

Experimental research primarily concentrated on observations of transitions of two-phase flow structures, which were initiated by variations of dielectrophoretic (DEP) force in the restrictor. In the analysis presented below, video recordings of vapour slugs moving along the microchannel were used together with synchronous measurements of differential pressure between the channel inlet and outlet. The (heated) microchannel was placed after the flow controller (restrictor), as shown in Fig. 2.

The video recordings were transformed into a black and white flow diagram showing the spatial and temporal evolution of the vapour bubbles and slugs in the observed microchannel. In the diagram, an example of which can be seen in Fig. 3, white regions represent portions of the channel

occupied by the vapour and the black areas represent segments filled with liquid. The horizontal coordinate indicates the observation time, counted from the moment of voltage switch-on and covers two voltage on/off cycles, that is 40 s in total. In this interval, the voltage was applied for 10 s and then switched off for another 10 s. The vertical coordinate shows position along the microchannel, starting from its inlet. In such diagram, a bubble moving towards the channel outlet is represented by a white line inclined to the right with the inclination angle indicating the bubble velocity. The width of this line, measured in vertical direction, equals to the bubble diameter. In the case of the slugs, this width gives the slug length. Stationary bubbles or slugs are traced as horizontal white lines or bands.

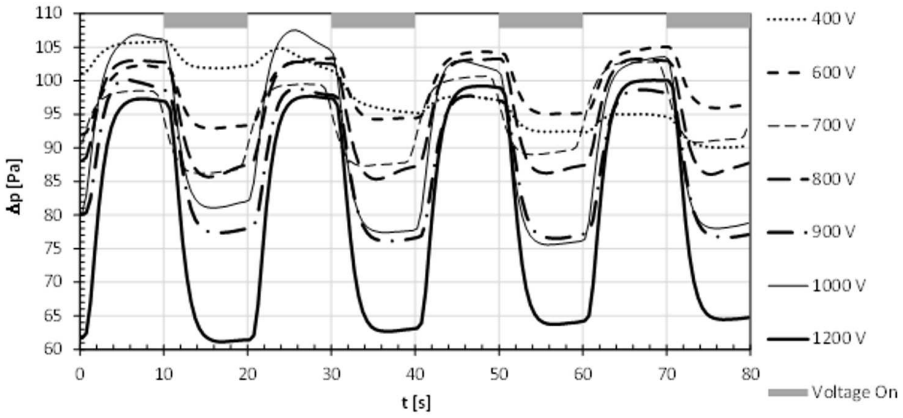

Figure 3: Profiles of differential pressure, Δp, measured between the heated microchannel ends for the syringe pump flowrate 0.05 ml/min and selected maximum values of voltage applied intermittently to the electrodes of the DEP restrictor.

Experimental observations were conducted for a number of the syringe pump flowrate values and voltages applied to the DEP restrictor electrodes. In Figs. 3 and 4, profiles of differential pressure, Δp, measured between the heated microchannel ends are shown for the syringe pump flowrates 0.05 and 0.2 ml/min and different maximum values of voltage applied intermittently to the electrodes of the DEP restrictor. In these figures, the time intervals of 10 s duration when the voltage was switched on are indicated by the grey bars. It is seen that switching the DEP voltage on causes the a sudden drop in Δp, which is deepest for the highest values of the voltage. Switching off the voltage causes the Δp return to its previous high value. More detailed analysis of selected measurements is presented in Figs. 5 to 8

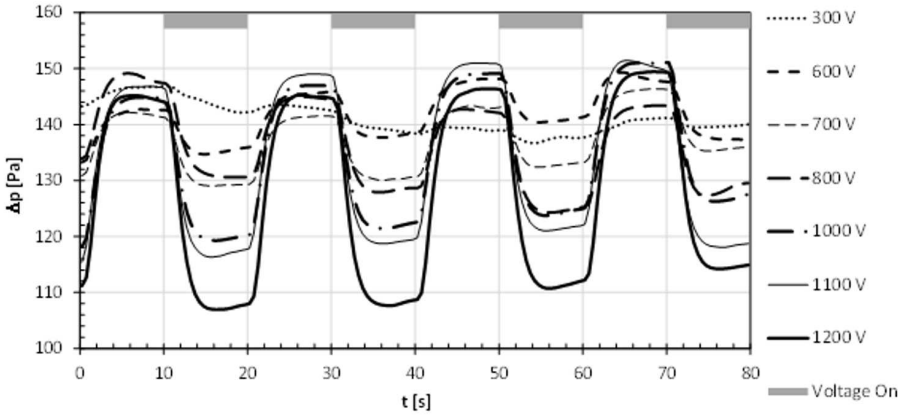

Figure 4: Profiles of differential pressure, Δp, measured between the heated microchannel ends for the syringe pump flowrate 0.2 ml/min and selected maximum values of voltage applied intermittently to the electrodes of the DEP restrictor.

for the flowrate of 0.05 ml/min and in Figs. 9 and 10 for the flowrate of 0.2 ml/min. The DEP voltage amplitude was increased before each subsequent measurement run, up to ±1200 V (2400 Vpp – peak-to-peak voltage).

Figure 5 shows the example of boiling flow in the microchannel with no DEP voltage applied. It may be seen in the flow diagram that most of the vapour bubbles originates from a nucleation site located in the channel at $x = 22$ mm. A few bubbles appear already at the channel inlet (at $t = 3.7$ s). They all move towards the channel outlet and grow up, transforming into vapour slugs in the middle part of the channel. As they approach the channel outlet, they partially condense. Average volume fraction in the entire microchannel, calculated from the flow diagram, is almost constant in time and approximately equals to 0.5. Measured differential pressure is also practically constant.

Periodical switching of voltage applied to the DEP restrictor disturbs the steadiness of the flowrate at the microchannel inlet and affects in this way the evolution of the vapour phase. It also results in periodical oscillations of the differential pressure and average void fraction. The latter is clearly distinguishable only for higher amplitudes of the voltage – see Figs. 6 and 7 for comparison. Regarding the flow structures, it can be seen that switching the voltage off causes acceleration in the bubbles/slugs movement. At the same time, the measured differential pressure increases. It is understood that switching the voltage off releases certain volume of

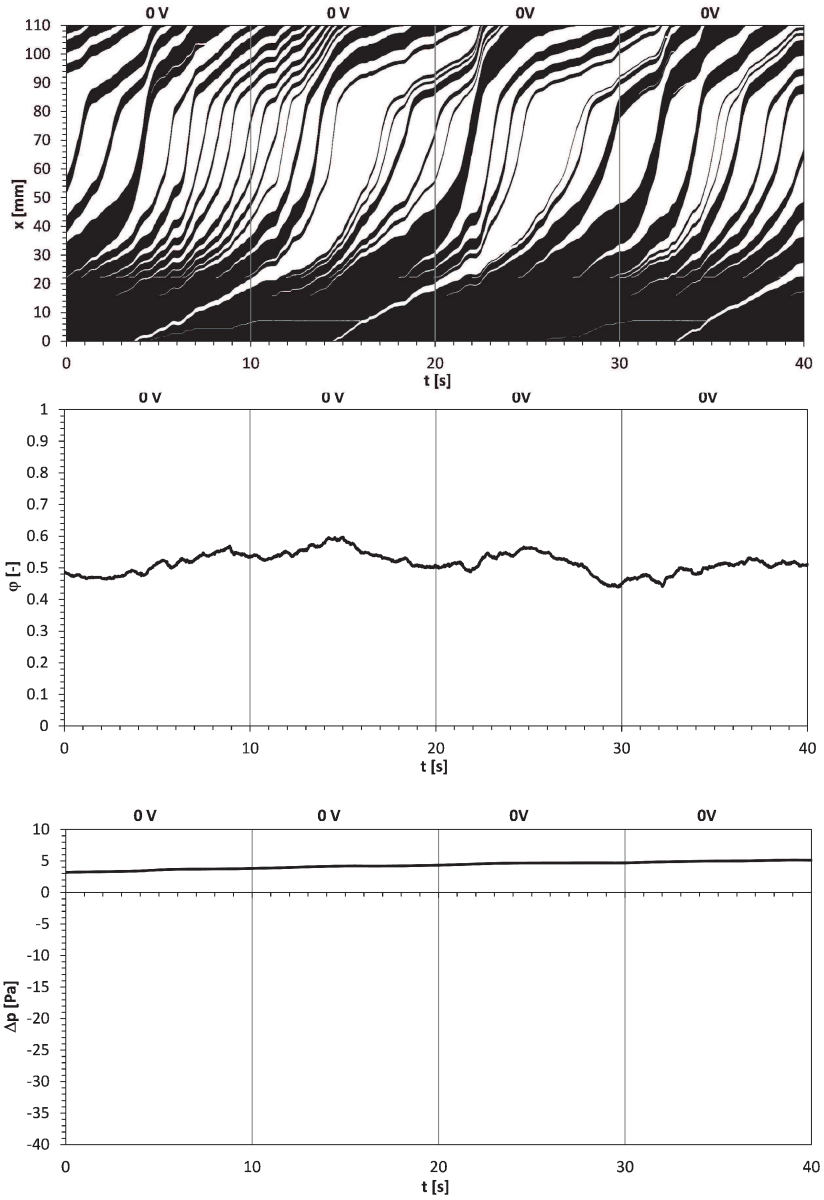

Figure 5: Boiling flow diagram (top), calculated average void fraction, φ, (middle) and differential pressure Dp between microchannel ends (bottom) measured for the syringe pump flowrate 0.05 ml/min and no voltage applied to the electrodes of the DEP restrictor.

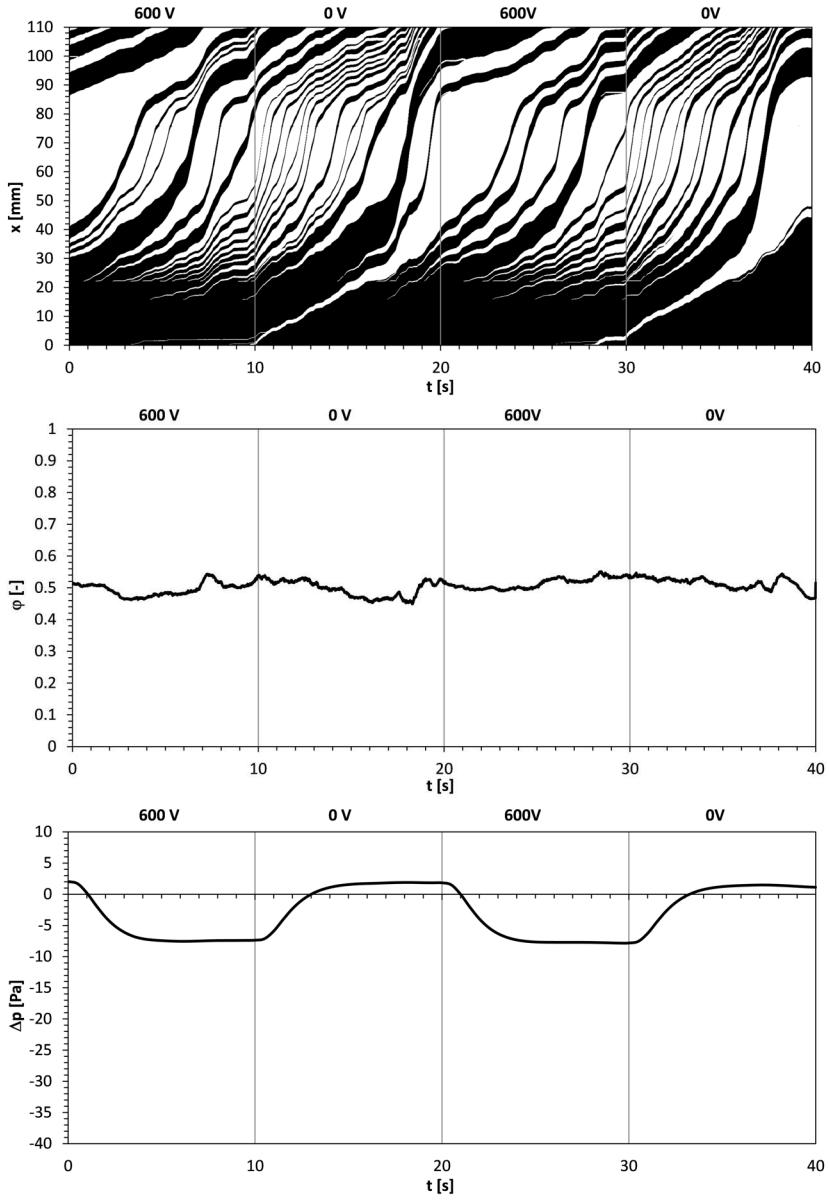

Figure 6: Boiling flow diagram (top), calculated average void fraction, φ, (middle) and differential pressure, Δp, between microchannel ends (bottom) measured for the syringe pump flowrate 0.05 ml/min and maximum voltage of ±600 V (1200 Vpp) applied to the electrodes of the DEP restrictor over a periods of 10 s.

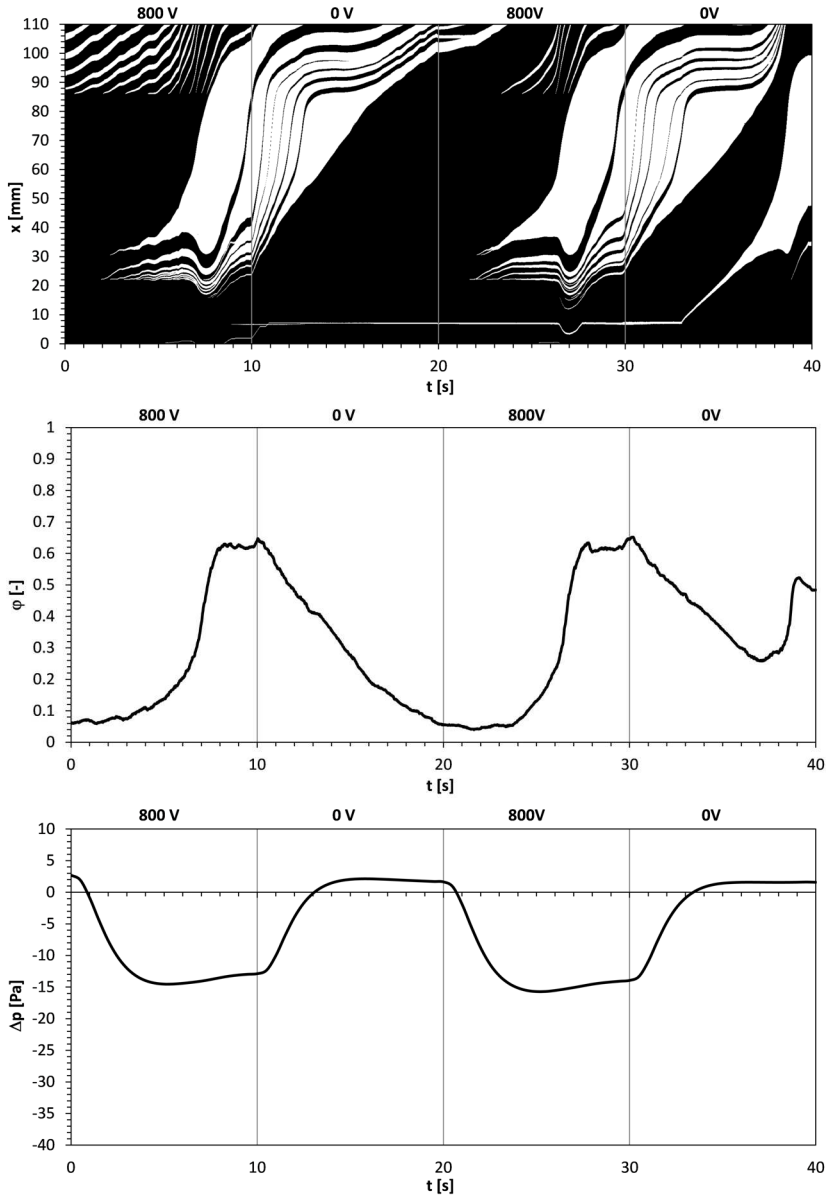

Figure 7: Boiling flow diagram (top), calculated average void fraction, φ, (middle) and differential pressure, Δp, between microchannel ends (bottom) measured for the syringe pump flowrate 0.05 ml/min and maximum voltage of ±800 V (1600 Vpp) applied to the electrodes of the DEP restrictor over a periods of 10 s.

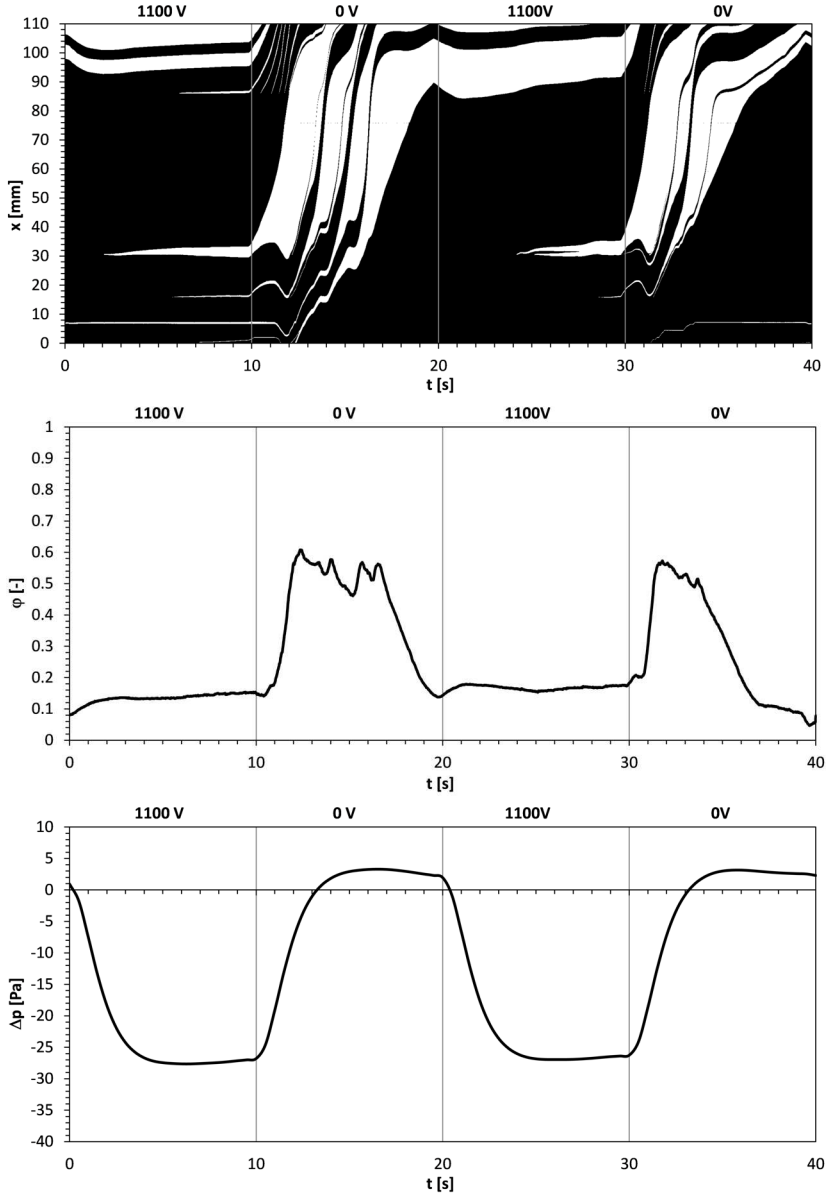

Figure 8: Boiling flow diagram (top), calculated average void fraction, φ, (middle) and differential pressure, Δp, between microchannel ends (bottom) measured for the syringe pump flowrate 0.05 ml/min and maximum voltage of $\pm$1100 V (2200 Vpp) applied to the electrodes of the DEP restrictor over a periods of 10 s.

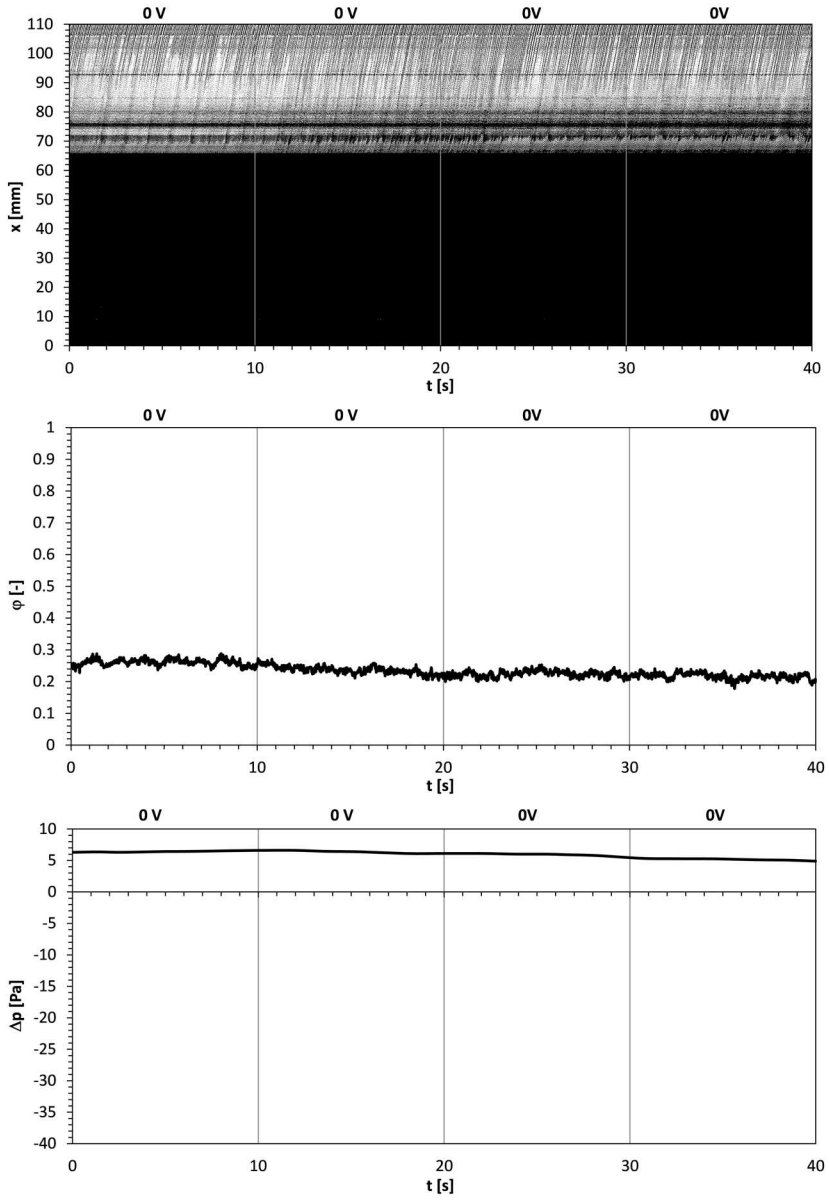

Figure 9: Boiling flow diagram (top), calculated average void fraction, φ, (middle) and differential pressure, Δp, between microchannel ends (bottom) measured for the syringe pump flowrate 0.2 ml/min and no voltage applied to the electrodes of the DEP restrictor.

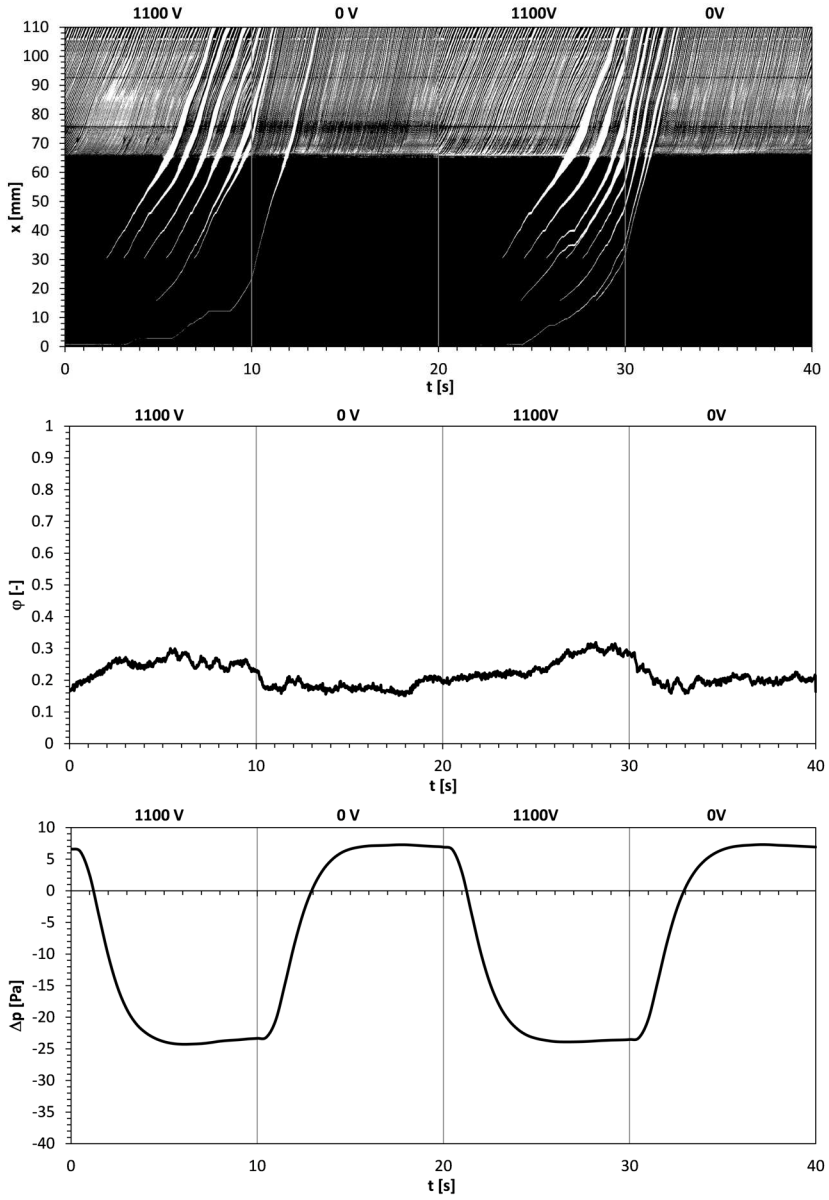

Figure 10: Boiling flow diagram (top), calculated average void fraction, φ, (middle) and differential pressure, Δp, between microchannel ends (bottom) measured for the syringe pump flowrate 0.2 ml/min and maximum voltage of $\pm$1100 V (2200 Vpp) applied to the electrodes of the DEP restrictor over a periods of 10 s.

liquid held by DEP forces in the restrictor. Subsequently, this liquid enters the microchannel, increasing there both the flow velocity and hydraulic resistance. When the voltage is applied again, the differential pressure diminishes. The effect of the DEP voltage alteration on the void fraction may be significant, as is shown in Figs. 7 and 8, but is ambiguous. For 800 V (Fig. 7), switching the voltage off causes partial condensation of the slugs in the microchannel, while for 1100 V (Fig. 8) opposite effect was observed. This is probably a result of heat losses in the outlet part of the microchannel. Due to these losses, the downstream part of the channel was colder than its middle part. Other curious effects are also observed for the 1100 V case. Namely, in the periods when the voltage was applied to the restrictor, the slugs in the microchannel remained almost stationary. Similar behaviour was also recorded with the DEP voltage of 900 V and 1200 V.

Investigations similar to these described above were repeated with the pump flow rate set at 0.2 ml/min. Example results for these series of experiments are shown in Figs. 9 and 10. With no voltage applied, the flow in the microchannel is stationary with small bubbles originating at short intervals from nucleation site at $x = 66$ mm. Periodic application of the DEP voltage induces differential pressure oscillations which are the same as for the corresponding previous runs with the flowrate of 0.05 ml/min. In the time intervals when the voltage is on, additional bubble generation was observed in the upstream half of the channel, principally at $x = 30$ mm. Calculated average void fraction was relatively low, amounting to about 0.25. Small increases may be noticed when the additional, larger bubbles move along the channel. Small amount of vapour phase indicates that the available heating power was too small to generate boiling flow over larger portion of the channel for the selected flowrate value. Nevertheless, a slight decrease of pressure induced by DEP restrictor was sufficient to trigger additional vapour generation.

The heat flux on the heated microchannel wall during the presented experiments was estimated from measured values of flowrate and average void fraction. According to [14], the isopropyl heat of vaporization equals to 663 kJ/kg. Thus, for the two values of flowrate used, the complete evaporation of saturated isopropyl requires the heat fluxes of 8.35 kW/m^2 and 33.4 kW/m^2, respectively. However, only a fraction of the liquid in the boiling microchannel was actually evaporated. Namely, the average void fraction was about 0.5 for the flowrate of 0.05 ml/min (see Figs. 5 and

6) or 0.25 for the runs with 0.2 ml/min (Figs. 9 and 10). Assuming no slip between the liquid and vapour phases, the dryness fraction (vapour mass fraction) is then estimated to amount to 0.003 and 0.001, respectively. Therefore, the actual heat flux on the microchannel wall amounted to 25 W/m^2 for the flowrate of 0.05 ml/min and 34 W/m^2 for 0.2 ml/min.

Differential pressure oscillations observed due to periodical DEP voltage switching were well repeatable and correlate with voltage magnitude. Namely, the amplitudes of the pressure and voltage oscillations are proportional to each other as shown in Fig. 11. It is seen that this relationship is independent of the pump flowrate.

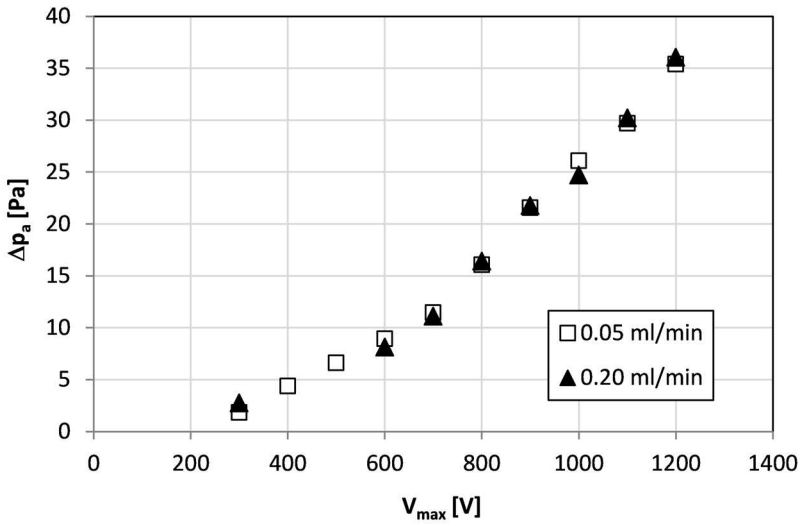

Figure 11: Amplitude of differential pressure oscillations, Δp_a, versus the maximum voltage V_{max} applied to the DEP restrictor electrodes for two values of the pump flowrate.

4 Conclusions

In the experiment presented here, dielectrophoretic restrictor was mounted upstream of the heated microchannel. The investigations focused on visual observations and recordings of vapour structures appearing in the microchannel boiling flow. In addition to video recordings, synchronous measurements of differential pressure were acquired. The measurements were made for a set constant liquid flowrate at the restrictor inlet. The influence

of the dielectrophoretic forces on the microchannel flow was investigated for various voltage values applied to the restrictor electrodes, reaching up to 2400 Vpp. The applied voltage was periodically switched on and off at time intervals of 10 s.

Operation of the dielectrophoretic restrictor principally influences the liquid flowrate at the microchannel inlet when the voltage applied to the restrictor electrodes is switched on or off. In effect hydraulic resistance of the flow also changes. As a consequence of these dynamic variations of the flow rate, vapour content in the boiling microchannel flow may be controlled. To achieve significant variation of the void fraction, applied voltage should be relatively high, i.e., of the order of ±1000 V (2000 Vpp). The experimental results of the measurements of the dielectrophoretic flow controller developed by the authors of this article are the first to show the effect of the presented device on the boiling process in the heated microchannel.

Acknowledgements This research has been supported by National Science Centre within the Project No. 2012/05/B/ST8/02742.

Received 20 October 2017

References

[1] Pethig R.: *Review article – dielectrophoresis: status of the theory, technology, and applications.* Biomicrofluidics **4**(2010), 2, 022811.

[2] Chakraborty D., Chakraborty S.: *Microfluidic Transport and Micro-scale Flow Physics: An Overview.* In: Microfluidics and Microfabrication, Springer, 2010, 1–85.

[3] Li M., Li W.H., Zhang J., Alici G., Wen W.: *A review of microfabrication techniques and dielectrophoretic microdevices for particle manipulation and separation.* J. Phys. D: Appl. Phys. **47**(2014), 6, 063001.

[4] Becker F.F., Wang X.-B., Huang Y., Pething R., Vykoukal J., Gascoyne P.R.: *Separation of human breast cancer cells from blood by differential dielectric affinity.* Proc. Natl. Acad. Sci. U.S.A. **92**(1995), 3, 860–864.

[5] Green N.G., Morgan H., Milner J.J.: *Manipulation and trapping of submicron bioparticles using dielectrophoresis.* J. Biochem. Biophys. Methods **35**(1997), 89–102.

[6] Pellat H.: *Force agissant á la surface de séparation de deux diélectriques.* CR Seances Acad. Sci. (Paris), **119**(1894), 675–678.

[7] Jones T.B.: *On the Relationship of Dielectrophoresis and Electrowetting.* Langmuir, **18**(2002), 11, 4437–4443.

[8] Jones T.B.: *Liquid dielectrophoresis on the microscale.* J. Electrostatics **51**(2001), 51-52, 290–299.

[9] Lackowski M., Krupa A., Butrymowicz D.: *Dielectrophoresis flow control in microchannels*. J. Electrostatics **71**(2013), 5, 921–925.

[10] Lackowski M.: *Dielectrophoresis flow control of volatile fluids in microchannels*. J. Therm. Sci. **24**(2015), 5, 1–5.

[11] Mikielewicz D., Klugmann M., Wajs J.: *Experimental investigation of M-shape heat transfer coefficient distribution of R123 flow boiling in small-diameter tubes*. Heat Transfer Eng. **33**(2012), 7, 584–595.

[12] Kuczyński W., Charun H., Bohdal T.: *Influence of hydrodynamic instability on the heat transfer coefficient during condensation of R134a and R404A refrigerants in pipe mini-channels*. Int. J. Heat Mass Transfer **55**(2012), 4, 1083–1094.

[13] Kuczyński W., Charun H.: *Modeling of a two-phase region length of the condensation of R134a and R404A refrigerants in pipe minichannels with periodic hydrodynamic in-stabilities*. Heat Transfer Eng. **35**(2014), 9, 850–862.

[14] Berman N.S, Larkam C.W., McKetta J.J.: *Vapor heat capacity and heat of vaporization of 2-propanol*. J. Chem. Eng. Data **9**(1964), 218–219.